DOI:10.1021/jf900851n

JOURNAL OF AGRICULTURAL AND FOOD CHEMISTRY
ARTICLE

Freeze-Dried Grape Powder Attenuates Mitochondria- and Oxidative Stress-Mediated Apoptosis in Liver Cells

Yumin Xu,[†,#] Vladimir I. Khaoustov,[†] Hui Wang,[†,#] Jing Yu,[†,⊥] Fazal Tabassam,[†] and Boris Yoffe*[,†,§]

[†]Department of Medicine, Baylor College of Medicine, Houston, Texas, [§]Michael E. DeBakey Veterans Affairs Medical Center, Houston, Texas, [#]Department of Infectious Disease, Ruijin Hospital, School of Medicine, Shanghai Jiaotong University, Shanghai, China, and [⊥]Department of Hepatology, First Affiliated Hospital of Guangxi, Guangxi Medical University, Nanning, Guangxi, China

The beneficial effects of grape consumption have been attributed to the antioxidant activity of its polyphenols. This study was conducted to investigate the cytoprotective effects of a freeze-dried grape powder (FDGP) on liver cells. FDGP treatment of primary hepatocytes and hepatoma cells revealed increased metabolic activity of cells and phosphorylation of Akt and IκBα, as well as up-regulation of proliferating cell nuclear antigen (PCNA) level. To study the molecular mechanisms of FDGP effects, cells were treated with TNF-related apoptosis-inducing ligand (TRAIL); taurodeoxycholic acid (TDCA); thapsigargin (TG), to induce cell apoptosis through death receptor-, mitochondria-, or ER-mediated pathway; and H_2O_2, to induce oxidative stress, respectively. TDCA-induced activation of caspase-3, caspase-7, caspase-9, and Bax was dramatically decreased with cotreatment of FDGP. Furthermore, FDGP reduced levels of annexin V positive cells by 4-fold. Also, FDGP pretreatment restored cellular glutathione content by 71% in cells treated with H_2O_2. However, FDGP did not inhibit ER-mediated apoptosis. In conclusion, FDGP increased the viability and metabolic activity of liver cells and attenuated oxidative stress- and mitochondria-mediated apoptosis. These data may contribute to the understanding of the mechanisms involved in protective effects of grape in a variety of liver conditions associated with cellular stress.

KEYWORDS: FDGP; liver cells; antiapoptotic effects of grape; apoptosis; oxidative stress; polyphenols

INTRODUCTION

Injury and death of parenchymal and nonparenchymal cells play key pathophysiological roles in the progression of liver disease. Activation of death receptors (Fas ligand, TNF-α), mitochondrial damage, and endoplasmic reticulum (ER) stress are the most important apoptotic pathways that induce liver injury (*1*, *2*). Imbalance between cell proliferation and cell death, resulting from activation or inhibition of signaling pathways, consequently leads to loss of tissue homeostasis and onset of pathologic conditions including liver diseases such as viral hepatitis, cholestatic liver disease, and steatohepatitis (*1*). Understanding the mechanisms involved in the disease process and prevention of cell death represents a long-term therapeutic goal. Therefore, it is important to identify new and effective drugs including alternative interventions that can prevent cell injury and cell death and promote cell regeneration.

Natural supplements and alternative medicine have attracted significant attention in recent years, in both the scientific and consumer communities for their health benefits for a variety of disorders, ranging from cancer to weight loss. As a result, the popularity of food additives has increased among consumers. A survey in liver clinics of six academic institutions revealed that 39% of patients with liver diseases used complementary and alternative medicine (*3*). Only recently have the potential health benefits of certain dietary supplements been confirmed by in vitro and in vivo studies (*4*−*7*). For example, several epidemiological studies have shown beneficial effects of green tea in cancer and cardiovascular diseases (*8*, *9*). Also, it has been demonstrated that coffee drinking may reduce the risk of liver cancer (*10*). Furthermore, dietary supplementation rich in polyphenols such as blueberries and apple juice showed neuroprotection for focal brain ischemia and Alzheimer's disease (*5*, *11*).

It is well-established that grapes and wine also have health-promoting effects (*12*). The "French paradox" refers to the low incidence of atherosclerotic cardiovascular disease despite a diet rich in total saturated fat, which is attributed to moderate daily drinking of red wine. Despite the potential risk for liver injury, there is indirect evidence suggesting that modest consumption of wine can be protective against liver injuries. A new study in mice suggested that the accumulation of fat in the liver caused by chronic alcohol consumption might be prevented by consuming resveratrol, a constituent of red wine (*13*). Also, resveratrol reduces steatosis in mice fed a high-calorie diet (*6*). Furthermore,

*Address correspondence to this author at VAMC, Bldg. 109, Room 139, 2002 Holcombe Blvd., Houston, TX 77030 [e-mail byoffe@bcm.tmc.edu; telephone (713) 794-7546; fax (713) 794-7870].

 Published on Web 09/16/2009

Table 1. Selected Phytochemicals in Freeze-Dried Grape Powder[a]

compound	μg/g (content ± SD)	compound	μg/g (content ± SD)
catechin	44 ± 3	quercetin	22 ± 1
epicatechin	23 ± 1	kaempferol	3.6 ± 0.2
anthocyanidins	106 ± 1	resveratrol	3.7 ± 0.1

[a] Freeze-dried grape powder (FDGP) was prepared and supplied by the California Table Grape Commission. LC-MS/MS determination of all FDGP compounds listed in **Table 1** was performed at the University of Illinois College of Pharmacy by using a Waters 2690HPLC system.

wine ameliorates many risk factors common to nonalcoholic fatty liver disease (NAFLD) and coronary heart disease such as insulin resistance and dyslipidemia (*14*). Indeed, modest wine consumption may reduce the prevalence of suspected NAFLD (*15*).

The beneficial health effects of grapes and red wine consumption have been attributed to the antioxidant activity of its polyphenols. In vivo animal studies showed that fresh grapes, rich in grape-specific polyphenols, directly protected both plasma low-density lipoprotein (LDL) and macrophages from oxidative stress and hence attenuated atherosclerosis development (*16*). Furthermore, resveratrol, at concentrations attainable after moderate wine intake, stimulates human platelet nitric oxide production via phosphoinositide-3-kinase (PI3K)-dependent protein kinase B (Akt), an integral component of cell signaling that regulates the survival pathway (*17*). Numerous previous studies using nonhepatic cell systems suggested that the individual grape compounds, such as procyanidins, resveratrol, catechins, flavanols, and anthocyanins, contain antioxidative, anti-inflammatory, antiapoptosis, antivirus, antiallergy, platelet antiaggregatory, and/or anticarcinogenic properties (*18*, *19*). However, there is limited evidence of how these grape compounds in combination might provide protective and beneficial effects on liver cells. Furthermore, it is conceivable that a combination of effective grape compounds might have more beneficial effects as compared to individual components to influence various intracellular signaling events. From a practical standpoint, a natural plant extract may contain numerous phytochemicals in balanced proportions, which may have superior abilities to interfere with multiple biochemical mechanisms. Therefore, a naturally balanced blend may be more beneficial than a single entity to oppose multiple toxic consequences (*20*).

The present study is performed to investigate the effects of a standardized freeze-dried powder made from fresh grapes (FDGP), rich in grape-specific polyphenols, on oxidative stress and apoptosis in liver cells.

MATERIALS AND METHODS

Grape Freeze-Dried Extract Preparation. A standardized FDGP was prepared and supplied by the California Table Grape Commission, and it is a composite of fresh red, green, and blue-black California grapes that have been frozen, ground with food-quality dry ice, freeze-dried, and reground using Good Manufacturing Practices for food product throughout. The powder was stored at −70 °C to preserve the integrity of biologically active compounds found in fresh grapes. One hundred grams of fresh grapes corresponds to approximately 18.2 g of powder. The composition of selected phytochemicals in FDGP was analyzed at the University of Illinois College of Pharmacy, Department of Medicinal Chemistry and Pharmacognosy as follows: FDGP samples (10.0 g) were refluxed with 40 mL of methanol/HCl (4 M aq) (4:1, v/v) for 30 min and, after cooling, the solutions were sonicated for 5 min. Aliquots of the sample solutions were diluted and mixed with internal standard (biochanin A) before LC-MS/MS analysis and analyzed by using HPLC (Waters 2690 HPLC system) and a Micromass (Manchester, U.K.) Quattro II triple-quadrupole mass spectrometer. The phytochemical analysis of FDGP is shown in **Table 1**.

For in vitro experiments FDGP was dissolved in DMSO as 10% stock solution. To establish optimal experimental conditions, cells were treated with different doses of increasing concentration of FDGP (from 0 to 2400 μg/mL) for different incubation times (up to 72 h). The same amount of DMSO (corresponding to a volume of 10% FDGP stock solution) was used in each control.

Cell Line and Culture. Human hepatoma cell line (Huh7) cells were cultured as described previously (*21*). Primary mouse hepatocytes (PMH) were obtained from Digestive Disease Core at Baylor College of Medicine (Houston, TX). Primary human hepatocytes (PHH) were purchased from In Vitro Technologies (Baltimore, MD). Primary hepatocytes were cultured in Williams' Medium E (Sigma, St. Louis, MO) supplemented with 10% fetal bovine serum, 1% penicillin−streptomycin−amphotercin B (Invitrogen, Carlsbad, CA), and 1% glutamine.

Drugs and Treatment Protocols. Recombinant human TNF-related apoptosis-inducing ligand (TRAIL) was purchased from Calbiochem (San Diego, CA). TRAIL is a member of TNF family, which induces cell apoptosis through the death receptor pathway. According to our titration results 400 ng/mL TRAIL (1 mg/mL stock solution in DMSO) was sufficient to induce death receptor-mediated apoptosis. Taurodeoxycholic acid (TDCA) was purchased from Sigma. TDCA (400 μM) was used to induce mitochondria-mediated apoptosis as previously described (*21*).

Thapsigargin (TG) is a Ca^{2+}-adenosine triphosphatase inhibitor and a disruptor of intracellular calcium homeostasis. TG (2 μM; Sigma) was used to induce ER-mediated apoptosis (*21*). H_2O_2 (0.8 mM; Sigma) was used to induce oxidative stress as described previously (*22*). LY294002 (LY), a specific inhibitor of PI3k-Akt signaling, was purchased from Cell Signaling (Beverly, MA). Unless otherwise stated, all other chemicals used in this study were obtained from Sigma. Untreated control cells were exposed to the same concentration of the solvents and were cultured and harvested in parallel with treated cells.

Morphological Analysis. Morphological examinations of treated and control cells were performed with phase-contrast microscopy and transmission electron microscopy. Additionally, identification of apoptosis in liver cells was performed with a single dye, 4′,6-diamidino-2-phenylindole (DAPI), as described previously (*23*). For electron microscope evaluation cells were collected and fixed with 2% formaldehyde and 3% glutaraldehyde in 0.1 mol/L sodium cacodylate buffer (pH 7.4) for 1 h at 4 °C. After fixation, cells were dehydrated in a graded series of acetone and embedded in epoxy resin. Ultrathin sections were cut, stained with uranyl acetate and lead citrate, and assessed using a JEOL 1200 EX electron microscope.

Cell Proliferation Analysis. A Cell Proliferation Kit was used according to the manufacturer's instructions (Roche Diagnostics, Indianapolis, IN). This quantitative colorimetric assay is based on the cleavage of the yellow tetrazolium salt 3-[4,5-dimethylthiazol-2-yl]-2,5-diphenyl tetrazoliumbromide (MTT) to purple formazan crystals by metabolic active cells.

Cell Death Detection. Apoptotic DNA fragmentation analysis was performed with a Cell Death ELISA kit according to the manufacturer's instructions (Roche Diagnostics). This assay is based on the quantitative sandwich enzyme immunoassay principle using mouse monoclonal antibodies directed against DNA and histones, respectively. This method allows the specific determination of mono- and oligonucleosomes in the cytoplasmic fraction of cell lysates.

Flow Cytometric Analysis of Annexin V−FITC Binding. To visualize phosphatidylserine externalization on the outer leaflet of the cellular membrane during apoptosis, treated and nontreated cells were cultured in 10 cm dishes, detached by trypsinization, resuspended, and washed in 1× annexin Hepes buffer (0.01 M Hepes, pH 7.4; 0.14 M NaCl; 2.5 mM $CaCl_2$; 2% FBS). Annexin V−FITC (Biosource, Camarillo, CA) was added (1 μL per 10^6 cells). Cells were incubated on ice for 30 min in the dark, washed twice, and resuspended with ice-cold annexin Hepes buffer. Propidium iodide (PI) was added to samples right before flow cytometry was performed. For each analysis 10000 events were recorded. Annexin V^+/PI^- cells were defined as early apoptotic, whereas annexin V^+/PI^+ cells were defined as late apoptotic. The early apoptotic cells were presented in the lower right quadrant of the fluorescence-activated cell sorting histogram, and the late apoptotic cells were present in the upper right quadrant; viable cells (both negative) and necrotic (only PI^+) cells, respectively, were present in the lower left and upper left quadrants.

Protein Analysis and Measurement of Caspase-3 Activity. The protein concentrations of the lysates were determined using a BCA protein assay kit (Pierce, Rockford, IL). Proteins were separated on sodium

dodecyl sulfate−polyacrylamide gel electrophoresis and transferred to nitrocellulose membranes (Bio-Rad Laboratories, Hercules CA). The blots were incubated with primary antibodies: caspase-9 (Calbiochem), phosphorylated inhibitory κBα (pI-κBα Ser32), phosphorylated-Akt (pAkt Ser473), phospho-p44/42 Map Kinase (pERK1/2), caspase-7 (Cell Signaling), Fas (Upstate, Lake Placid, NY), caspase-8, PCNA, Bax, cytochrome C (Santa Cruz Biotechnology, Santa Cruz, CA), PARP (R&D Systems, Minneapolis, MN), caspase-12 (ProSci Inc., Poway, CA), and Bip/GRP78 (BD Bioscience, San Diego, CA).

Immunoreactivity was detected by sequential incubation of horseradish peroxidase-conjugated secondary antibodies, and specific complexes were detected with the ECL system (GE Healthcare Bio-Sciences Corp., Piscataway, NJ). β-Actin was used as an internal control for the adjustment of protein loading. The relative intensity of bands was measured as described previously (*24*). For analysis of cytochrome C, mitochondrial and cytosolic fractionations were isolated using the Mitochondrial Fractionation Kit according to the manufacturer's instructions (Active Motif, Carlsbad, CA). For Western blot analysis of NF-κB, nuclear extracts were prepared as previously described (*25*).

Caspase-3 activity was measured using a Caspase-3 Cellular Activity Assay Kit according to the manufacturer's instructions (Calbiochem).

Silencing Akt Expression. To down-regulate Akt expression, cells were transfected with Akt siRNA kit (Cell Signaling Technology) according to the manufacturer's instructions. Briefly, cells were grown in 6-well plates for 24 h and at 80% confluence were transfected with negative control siRNA or Akt-specific siRNA. After transfection, cells were cultured for 3 days followed by treatment with or without FDGP for 24 h, and then the cell lysates were analyzed by Western blot.

Determination of Glutathione Content. The glutathione contents in cell lysates were measured by a Glutathione Assay Kit according to the manufacturer's instruction (Cayman Chemical, Ann Arbor, MI). This kit utilizes an enzymatic recycling method, using glutathione reductase, for the quantification of glutathione. The sulfhydryl group of glutathione reacts with 5,5′-dithiobis(2-nitrobenzoic acid) and produces a yellow-colored 5-thio-2-nitrobenzoic acid.

Statistical Analysis. The statistical significance of the difference between the results was analyzed with ANOVA and Student's *t* test. Differences were considered to be significant when the *P* value was < 0.05.

RESULTS

Effect of FDGP on Cell Proliferation and Regulation of Intracellular Signaling. The FDGP titration revealed dose-dependent modulation of cell proliferation (**Figure 1a**). To examine the cytoprotective effects of grape, treatment with 300 μg/mL FDGP was chosen for both primary hepatocytes and the hepatoma cell line. The assessment of the levels of proliferating cell nuclear antigen (PCNA), a marker of cellular proliferation, revealed that FDGP treatment stimulates the expression of PCNA (**Figure 1b**).

It was suggested that both Akt and extracellular regulated kinase (ERK) are involved in the regulation of cell growth, apoptosis, and survival pathways (*26*). Our results demonstrated that the level of Akt phosphorylation was increased by 2.24-fold following treatment with 300 μg/mL FDGP (**Figure 1b**). Additionally, phosphorylation of IκBα (a downstream effector of Akt) was increased by 2.36-fold (**Figure 1b**). Furthermore, FDGP also slightly increased the phosphorylation of ERK1/2 (by 1.15-fold).

To further investigate the role of the Akt pathway in the cytoprotective effect of FDGP, a specific inhibitor of the PI3K/Akt kinase pathway, LY294002 (LY), was used. The results demonstrated that treatment with 50 μM LY for 24 h totally blocked the phosphorylation of Akt (**Figure 1c**). These results were confirmed with Akt siRNA experiments, demonstrating that it suppresses FDGP-induced phosphorylation of Akt (**Figure 1d**). Additional tests were performed to evaluate cell viability (by trypan blue exclusion) after 24 h of treatment with either FDGP alone or FDGP in combination with LY. Cell viability in untreated (control) and FDGP-treated cells was 91 and 92%, respectively.

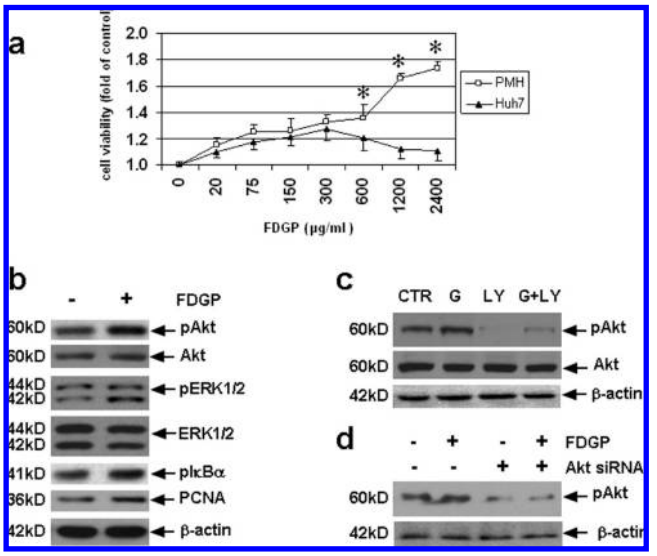

Figure 1. Effect of FDGP on cell proliferation and intracellular signaling. (**a**) Primary mouse hepatocytes (PMH) and Huh7 cells were cultured in 96-well plates (15000 cells/well) and treated with titrated doses of FDGP (from 0 to 2400 μg/mL) for 24 h and analyzed with an MTT Cell Proliferation Kit according to the manufacturer's instructions (Roche). Data are presented as fold of control. Each bar represents the mean ± SD of three independent assays in concentration determination studies (∗, $P < 0.05$); each assay was done in triplicate. (**b**) Primary mouse hepatocytes were treated with or without FDGP 300 μg/mL for 24 h. Cell lysates were analyzed by Western blot with antibodies specific for PCNA, Akt phosphorylated at serine 473 (pAkt), IκBα phosphorylated at serine 32 (pIκBα), and Map Kinase phosphorylated at Thr202/Tyr204 (pERK1/2). β-Actin was assessed for adjustment of protein loading. Total protein per lane is 30 μg. Results are representative of three independent experiments. (**c**) Huh7 cells were untreated (CTR) or treated with 300 μg/mL FDGP (G), 50 μM LY294002 (LY), or a combination of FDGP and LY (G+LY) for 24 h. Cell lysates were analyzed by Western blotting with antibodies specific for Akt phosphorylated at serine 473 (pAkt). β-Actin was assessed for adjustment of protein loading. Total protein per lane is 30 μg. Results are representative of three independent experiments. (**d**) Western blot analysis of Huh7 cells transfected (+) or not (−) with Akt siRNA. Antibodies for Akt phosphorylated at serine 473specific (pAkt) were used. The Akt siRNA suppresses the FDGP-induced phosphorylation of Akt. β-Actin was assessed for adjustment of protein loading. Results are representative of three independent experiments.

Treatment with LY alone decreased cell viability to 39%, and LY in combination with FDGP decreased cell viability to 41% (data not shown). Taken together, these results indicate that FDGP might increase cell survival and proliferation through the involvement of the Akt/PKB signaling pathway.

Effect of FDGP on Mitochondria-Mediated Apoptosis Induced by TDCA. Cells were treated with FDGP 300 μg/mL alone or in combination with increasing (from 50 to 800 μM) concentrations of TDCA. The MTT assay results showed that TDCA alone decreased the cell viability dose dependently. Interestingly, cotreatment with FDGP restores cell viability (**Figure 2a**). Phase contrast (**Figure 2b**) and transmission electron microscopy (**Figure 2c**) revealed that both untreated cells and FDGP-treated cells displayed normal morphology, whereas TDCA-treated cells exhibited the morphological characteristics of apoptosis including decreased number of adherent cells, reduced cytoplasmic extensions, small nucleus, loss of microvilli in plasma membrane, fragmentation and condensation of the nuclear chromatin, vacuolization in the cytoplasm, membrane blebbing, cell shrinkage, and dissolution of

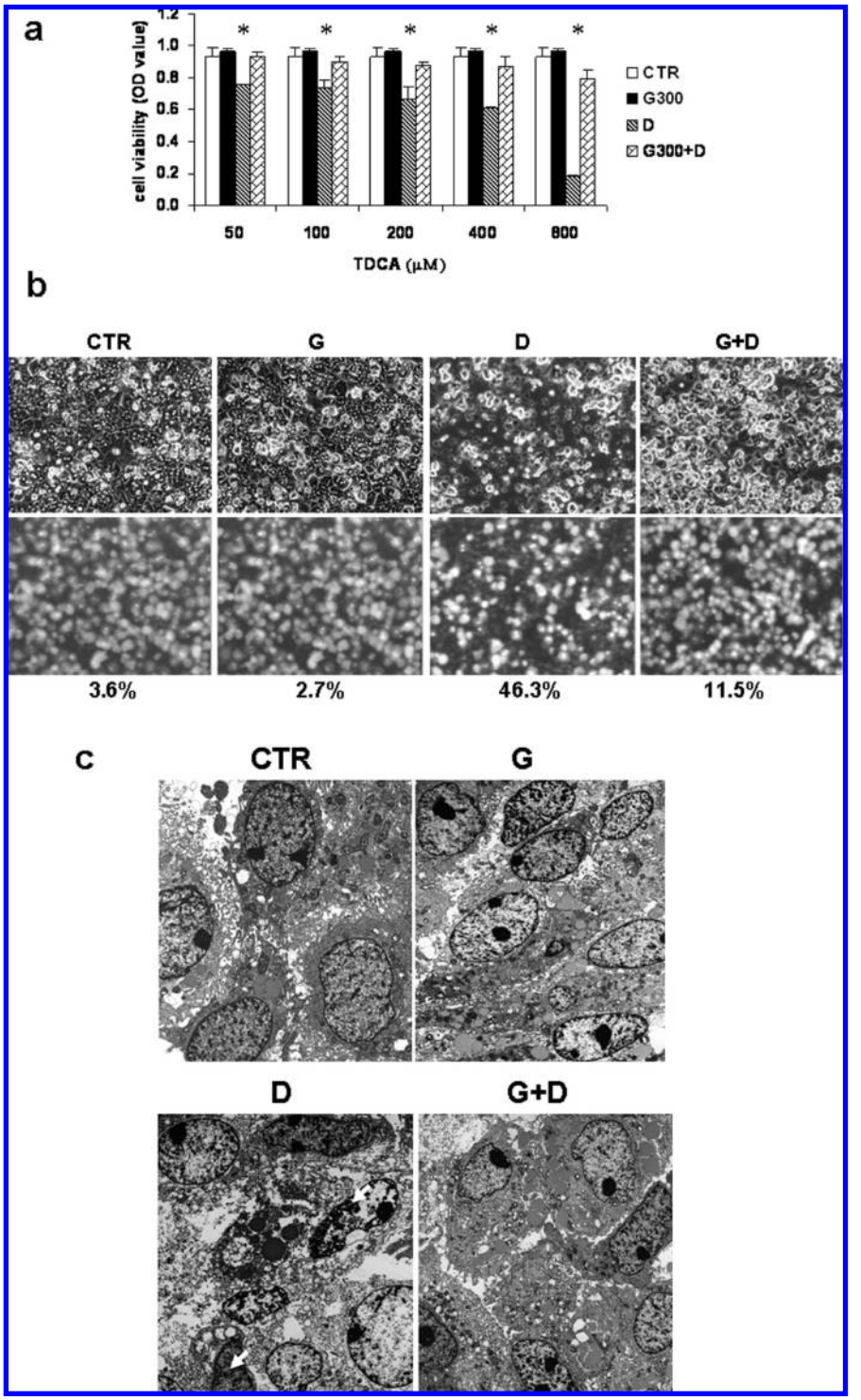

Figure 2. Morphological and metabolic assessment of the effect of FDGP on TDCA-induced apoptosis. (**a**) Primary mouse hepatocytes were treated with FDGP 300 μg/mL and/or different concentrations of TDCA for 24 h. Cell viability was measured by using the MTT assay. Data are presented as fold of control. At each concentration of TDCA, analysis of variance was used to compare the four experimental conditions (CTR, control; G300, FDGP; D, TDCA; G300+D, combination of FDGP and TDCA). D was found to be significantly different from each of the conditions ($*$, $P < 0.05$). There were no statistically significant differences between any the other three conditions (CTR, G300, and G300+D). Each bar represents the mean $\pm$ SD of three independent assays; each assay was done in triplicate. (**b**) Effect of FDGP on cell morphological alterations. Primary mouse hepatocytes were untreated (CTR) or treated with FDGP 300 μg/mL (G), 400 μM TDCA (D), and a combination of both (G+D) for 24 h. Cell morphology was observed under phase contrast microscopy (top panel) and fluorescent microscopy after DAPI staining (middle panel). The quantification of positive DAPI staining is shown as percent of apoptotic cells (bottom panel). (**c**) Electron microscopic evaluation of TDCA-treated Huh7 cells. Untreated cells (CTR) or FDGP-treated cells (G) displayed normal morphology. TDCA-treated cells (D) showed the morphological characteristics of apoptosis including loss of microvilli in plasma membrane, fragmentation and condensation of the nuclear chromatin (white arrows), and vacuolization in the cytoplasm as well. Co-incubation of TDCA with FDGP (G+D) improved the integrity of subcellular organelles and abolished morphological changes. Results are representative of three independent experiments. Original magnification, $\times$2500.

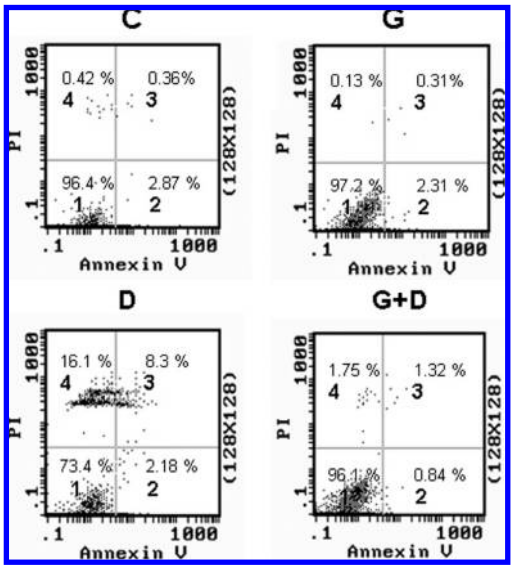

Figure 3. Flow cytometry analysis of the effect of FGDP on TDCA-induced apoptosis. Huh7 cells were untreated (C) or treated with 300 μg/mL FDGP (G), 400 μM TDCA (D), or a combination of FDGP and TDCA (G+D) and stained with annexin V and PI. The early apoptotic cells are presented in the lower right quadrant [2] of the fluorescence-activated cell sorting histogram. The late apoptotic cells are presented in the upper right quadrant [3]. Viable cells (both negative) and necrotic (only PI+) cells, respectively, are shown in the lower left [1] and upper left [4] quadrants. Results are representative of three independent experiments.

nuclear lamina. Cotreatment with FDGP improved the integrity of subcellular organelles and diminished the morphological changes. Furthermore, DAPI staining confirmed that cotreatment with FDGP decreased TDCA-induced apoptosis by 4.5-fold (**Figure 2b**). Similarly, the flow cytometry analysis demonstrated that the number of annexin V and PI double-positive cells significantly increased following treatment with TDCA alone; however, this apoptotic cell population was decreased by 6.3-fold when cells were cotreated with FDGP (**Figure 3**).

To understand the underlying signaling mechanisms involved in FDGP-mediated cell proliferation and cell survival, we performed Western blot analysis of cells treated with FDGP alone or in the combination with TDCA. Our results revealed that TDCA treatment induced up-regulation of Bax; however, FDGP cotreatment reduced this effect and normalized the level of Bax expression (**Figure 4a**). Also, in the presence of TDCA the amount of cytochrome C was markedly increased in the cytosolic fraction, whereas in the mitochondrial fraction it was decreased. Cotreatment with FDGP reduced release of cytochrome C in cells (**Figure 4**). Additionally, TDCA resulted in processing of procaspase-9 with the formation of a 37 kDa cleaved protein and subsequent processing of caspase-7 with the formation of a 20 kDa cleaved protein, as well as the cleavage of PARP, which is an intracellular substrate of caspase-3 protease. Cotreatment with FDGP abolished activation of caspase-9 and -7 and cleavage of PARP (**Figure 4a**). Furthermore, measurement of caspase-3 activity revealed that the TDCA treatment increased the activation of caspase-3 by 4.4-fold, but cotreatment with FDGP decreased the activation by 1.2-fold (**Figure 4b**). The levels of PCNA, pAkt, and pIκBa were decreased with TDCA

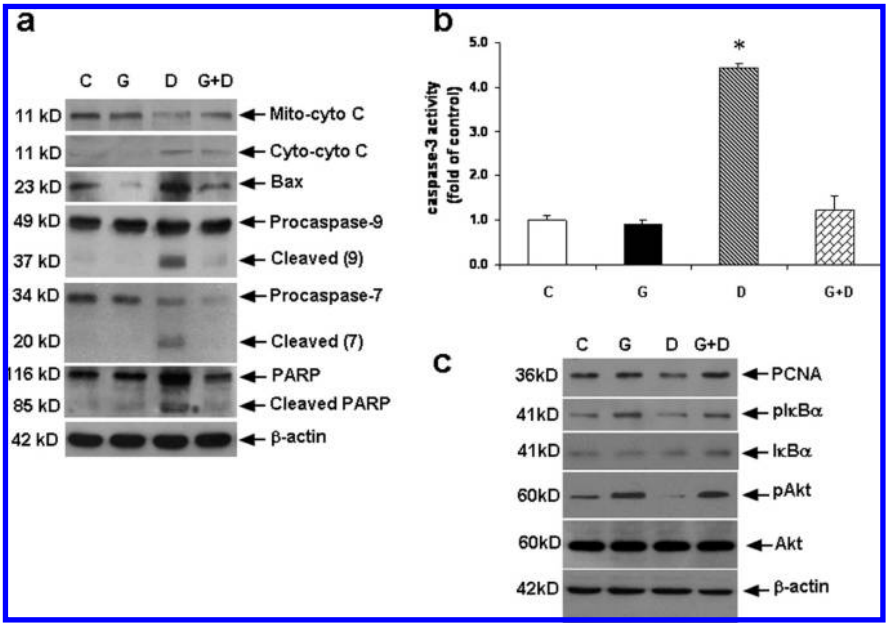

Figure 4. Western blot analysis and caspase-3 activity assay of the effect of FDGP on TDCA-induced apoptosis. (**a**) Huh7 cells were treated or untreated for 48 h with FDGP 300 μg/mL and/or 400 μM TDCA. Cell lysates were analyzed by immunoprecipitation and Western blot for markers of apoptosis involved in mitochondria pathway: Bax, caspase-9, caspase-7, PARP, and cytochrome C. Mito-cyto C, cytochrome C in mitochondrial fractionation; Cyto-cyto C, cytochrome C in cytosolic fractionation. β-Actin was used to confirm equal loading of proteins. Total protein per lane is 40 μg. C, control; G, FDGP; D, TDCA; G+D, combination of FDGP and TDCA. (**b**) Primary human hepatocytes were untreated (C) or treated with 300 μg/mL FDGP (G), 400 μM TDCA (D), or a combination of FDGP and TDCA (G+D). Caspase-3 cellular activity assay was performed according to the manufacturer's instructions. Graph represents the fold activation of treated cells over untreated control ones. Analysis of variance was used to compare the four experimental conditions (C, G, D, and G+D). D was found to be significantly different from each of the other conditions ($*$, $P < 0.05$). There were no statistically significant differences between any the other three conditions (C, G, and G+D). Each bar represents the mean $\pm$ SD of three independent assays; each assay was done in triplicate. (**c**) Primary mouse hepatocytes were treated or untreated with FDGP 300 μg/mL and/or 400 μM TDCA for 24 h. Cell lysates were analyzed by Western blotting with specific antibodies for Akt phosphorylated at serine 473 (pAkt), IκBα phosphorylated at serine 32 (pIκBα), and PCNA. β-Actin was assessed for adjustment of protein loading. Total protein per lane is 40 μg. C, control; G, FDGP; D, TDCA; G+D, combination of FDGP and TDCA treatment. Results are representative of three independent experiments.

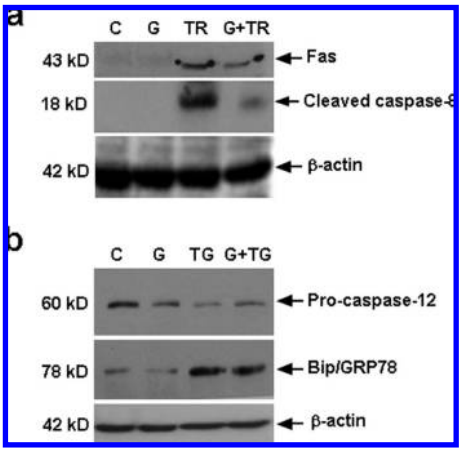

Figure 5. Effects of FDGP on death receptor-mediated and ER stress-mediated apoptosis. Huh7 cells were untreated or treated for 48 h with 300 μg/mL FDGP and/or 400 ng/mL TRAIL (**a**) or 2 μM TG (**b**). Cell lysates were analyzed by Western blotting with antibodies specific for Fas, cleaved caspase-8, Pro-caspase-12, and Bip/GRP78. β-Actin was used to confirm equal loading of proteins. Total protein per lane is 40 μg. C, control; G, FDGP; TR, TRAIL; TG, thapsigargin; G+TR, combination of FDGP and TRAIL; G+TG, combination of FDGP and TG. Immunoblots are representative of three independent experiments.

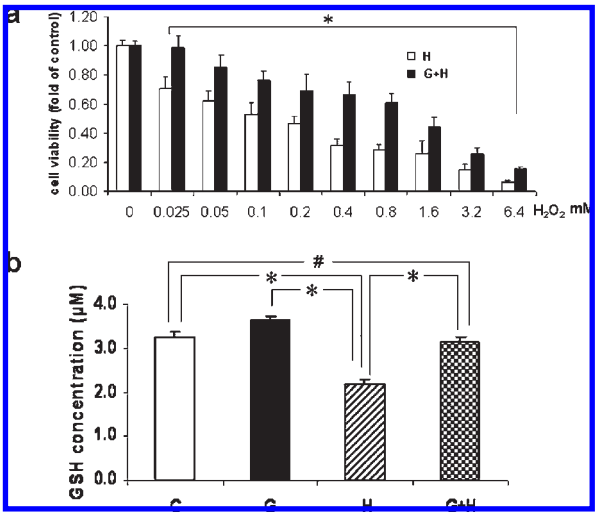

Figure 6. Reduction of H_2O_2-induced oxidative stress by FDGP treatment. (**a**) Huh7 cells were pretreated with 300 μg/mL FDGP or nontreated for 23 h and then incubated with different doses of H_2O_2 for 1 h. Cell viability was analyzed using MTT assay. H, cells were treated for 1 h with H_2O_2; G+H, cells pretreated for 23 h with 300 μg/mL FDGP were treated for 1 h with H_2O_2 and FDGP simultaneously. Each bar represents the mean $\pm$ SD of three independent assays; each assay was done in triplicate. $*$, $P < 0.05$. (**b**) Huh7 cells were treated with 300 μg/mL FDGP for 23 h or nontreated and then incubated with 0.8 mM of H_2O_2 for 1 h. Intracellular glutathione (GSH) content was measured by using s GSH Assay kit. C, untreated cells as a control; G, treated with FDGP; H, treated with H_2O_2; G+H pretreated with FDGP for 23 h and then incubated for 1 h with H_2O_2 and FDGP simultaneously. $*$, $P < 0.05$; #, $P > 0.05$. Each bar represents the mean $\pm$ SD of three independent assays; each assay was done in triplicate.

treatment, but they were all up-regulated by co-incubation of FDGP (**Figure 4c**). Taken together, our data indicate that FDGP is able to attenuate the mitochondria-mediated apoptosis induced by TDCA.

Effect of FDGP on ER and Death Receptor Pathways of Apoptosis. To examine the cytoprotective effects of FDGP on other apoptotic pathways, cells were treated with TRAIL and TG to induce apoptosis through death receptor and ER stress pathways, respectively. Treatment with TRAIL led to up-regulation of Fas and cleavage of procaspase-8, which was alleviated by treatment with FDGP. Following treatment with TG, activation of procaspase-12 and Bip/GRP78 was observed. However, no changes were found in the expression of caspase-12 and Bip/GRP78 in cells treated with TG in combination with FDGP (**Figure 5**). These data suggest that FDGP is able to ameliorate apoptosis through the death receptor pathway, but may not be able to prevent ER-mediated apoptosis.

Effect of FDGP on H_2O_2-Induced Oxidative Stress. It has been suggested that loss of glutathione and oxidative damage is an early event in the apoptotic program (*20*, *22*). To investigate the antioxidative properties of FDGP, we used H_2O_2 to induce oxidative stress in cells. The H_2O_2 titrations revealed dose-dependent induction of cell death that was increased by 40% at dose of 0.1 mM H_2O_2 and by 95% at 6.4 mM H_2O_2. Therefore, an H_2O_2 concentration of 0.8 mM was chosen as optimal for induction of oxidative stress (**Figure 6a**). To investigate the free radical scavenging abilities of FDGP, cells were pretreated with FDGP for 23 h following incubation for 1 h with 0.8 mM H_2O_2 and FDGP simultaneously, and then the levels of glutathione were measured. The glutathione content in FDGP-untreated cells (control) significantly decreased after H_2O_2 treatment. However, pretreatment cells with FDGP dramatically abolished the H_2O_2 effect (**Figure 6b**), and glutathione content remained nearly at normal levels ($P < 0.05$). These data indicated that FDGP inhibited the H_2O_2-induced oxidative stress.

DISCUSSION

The biological, pharmacological, and therapeutic properties of plant polyphenols have attracted increased interest from the scientific community (*7*, *12*, *13*, *16*, *18*−*20*). Recent studies demonstrated that grape polyphenols reduced macrophage atherogenicity in mice, ameliorated cerebral ischemia-induced neuronal death in gerbils, and exhibited a cardioprotective effect in human (*16*, *27*, *28*). Furthermore, both resveratol and anthocyanin increased the life span both in mice fed a high-fat diet and in cancer-susceptible Trp53(−/−) mice, respectively (*6*, *29*). The most striking observation of the first study was the ability of resveratrol to protect mice against development of hepatic steatosis or fatty liver, a condition commonly associated with obesity and insulin resistance (*6*). These as well as other studies clearly demonstrated that grape individual compounds, such as resveratrol, procyanidins, catechins, flavanols, and anthocyanins, may exhibit antioxidative, anti-inflammatory, antiapoptosis, antivirus, antiallergy, platelet antiaggregatory, and/or anticarcinogenic properties (*18*, *19*). However, there is limited evidence of how these grape compounds may work in combination to provide protective or beneficial effects. It is possible that these naturally balanced compounds possess greater beneficial effects compared to each individual compound. This phenomenon may explain the reason for lack of beneficial effects in clinical studies with other antioxidants such as vitamins C and E and β-carotene (*30*).

In addition, it has been demonstrated that some grape compounds may exhibit dissimilar effects toward human cancer and normal cells (*18*, *19*). For example, anthocyanidin demonstrates different time- and dose-dependent cytotoxic effects in human breast, lung, and gastric adenocarcinoma cells, whereas under similar conditions this compound enhanced the growth and viability of normal cells (*7*). An analogous effect was demonstrated with *S*-adenosylmethionine (dietary supplement), which may inhibit the apoptosis of normal hepatocytes and stimulate

the apoptosis of liver cancer cells (*31*). Our experiments showed that FDGP at the dose of 300 μg/mL stimulated growth and viability of normal hepatocytes but did not induce apoptosis in hepatoma cells, Huh7. This phenomenon may be associated with the doses of bioactive compounds of FDGP. It was reported that the effective dose of resveratrol that induces apoptosis in tumor cells ranges from 40 to 200 μM (*18*, *19*). In our case, FDGP-adjusted doses of pro-apoptotic compounds such as resveratrol and cyanidin were 1000 times less.

Apoptosis plays a critical role in the pathogenesis of liver diseases. Activations of death receptors, mitochondrial damage, and ER stress are the most important apoptotic pathways that induce liver injury (*1*, *2*). Preventing liver cell apoptosis may lead to the prevention of various liver diseases. Mitochondria are pivotal in controlling cell life and death. The central roles for mitochondria as the orchestrators of apoptosis have been well established (*32*). In this study TDCA was used to induce apoptosis through the mitochondria pathway. Treatment with FDGP significantly reduced annexin V positive apoptotic cell population as well as the number of positive DAPI-stained cells. Electron microscopy revealed that cotreatment with FDGP reduced TDCA-induced morphological apoptotic alterations of cytoplasm and nuclei, including membrane blebbing, cell shrinkage, and dissolution of nuclear lamina. Apoptosis is associated with the externalization of phosphatidylserine on the outer leaflet of the cellular membrane during apoptosis, which features "eat me" signals on the surface of the apoptotic cell that make it recognizable by specific macrophage receptors (*33*). The relocalization of the Bax protein from the cytoplasm to the outer mitochondrial membrane and the subsequent release of cytochrome C initiate apoptosis following activation of caspase-9 and subsequent processing of executive caspase-3 and -7 (*32*). Cytosolic cytochrome C forms an essential part of the vertebrate "apoptosome", which is composed of cytochrome C, Apaf-1, and procaspase-9. Caspase-3 and -7 are the key executioners of apoptosis. Both of them are partially or totally responsible for the proteolytic cleavage of many key proteins such as the nuclear enzyme PARP (*34*). Cleavage of PARP by effector caspases constitutes a hallmark of apoptosis. Our data showed that treatment with FDGP inhibits TDCA-induced mitochondria-associated apoptotic events such as overexpression of Bax, increased release of cytochrome C from mitochondria, and sequent activation of caspase-9, -7, and -3 and PARP.

To gain additional insight into the molecular mechanism of FDGP cytoprotective effects, we also analyzed the involvement of Akt pathway. The Akt/PKB signaling pathway functions as a critical regulator of cell survival and proliferation (*26*). The activation of Akt pathway provides cells with a survival signal that allows them to withstand apoptotic stimuli. NF-κB is known as a downstream mediator of Akt in antiapoptotic signaling (*35*). When bound to its cytotoxic inhibitor, I-κB, NF-κB is sequestered in the cytoplasm. Upon its phosphorylation by I-κB kinase, I-κB is degraded, which allows NF-κB to move to the nucleus and activate the transcription of antiapoptotic proteins. Phosphorylation at Akt/PKB serine 473 may cause NF-κB activation and induce cell proliferation. Our findings demonstrated that treatment with FDGP increased the phosphorylation of both Akt and IκB. Silencing Akt expression with Akt-specific siRNA or cell pretreatment with a pharmacologic inhibitor of Akt signaling pathway (LY) almost abolished the FDGP-induced Akt phosphorylation. Additionally, we found that treating cells with FDGP induced expression of PCNA. This protein is associated with cell cycle progression. Taken together, our results suggested that FDGP-induced cell growth and proliferation are associated with the Akt/ NF-κB cell survival pathway.

Execution of the apoptotic program triggered by both oxidant and nonoxidant stimuli may be associated with the production of reactive oxygen species and resultant oxidative stress (*33*). The glutathione redox cycle provides cellular protection against free radicals (*22*). Loss of glutathione and oxidative damage are the early signaling events of apoptosis (*20*). We demonstrated that treatment with H_2O_2 led to glutathione depletion, thus altering the cellular redox status by overproduction of free radicals. However, preincubation with 300 μg/mL FDGP prevented reduction of glutathione content in cells subsequently treated with H_2O_2. These data suggest that FDGP protects against oxidative injury. Taken together, we propose that the cytoprotective effects of FDGP were predominantly associated with the reduction of oxidative stress and prevention of mitochondrial injury.

Furthermore, the ability of FDGP to protect cells from apoptosis associated with either ER stress or death receptors was examined. The results showed that treatment with FGDP slightly reduced TRAIL-induced apoptosis, but it does not affect ER stress-mediated apoptosis.

In summary, FDGP promotes liver cell viability, proliferation, and metabolic activity, which is associated with the Akt survival pathway, prevents H_2O_2-induced oxidative cell damage, restores intracellular glutathione content, and ameliorates mitochondria-mediated and death receptor-mediated apoptosis. However, FDGP did not prevent ER stress-mediated apoptosis induced by TG. These data may contribute to our understanding of the molecular mechanisms involved in protective effects of grape in a variety of liver conditions associated with oxidative cell injury and apoptosis. Moreover, with further development of nutrigenomics, on the basis of a simple gene test, physicians can personalize "food medicine", which makes it possible for patients to control their weight, optimize their health, and reduce the risk of cancer, diabetes, and liver diseases.

ABBREVIATIONS USED

FDGP, freeze-dried grape powder; TDCA, taurodeoxycholic acid; TG, thapsigargin; ROS, reactive oxygen species; TRAIL, TNF-related apoptosis-inducing ligand; MTT, 3-[4,5-dimethylthiazol-2-yl]-2,5-diphenyltetrazolium bromide; PARP, poly(ADP-ribose) polymerase; PCNA, proliferating cell nuclear antigen; IκBα, NF-κB inhibitor-α.

LITERATURE CITED

(1) Guicciardi, M. E.; Gores, G. J. Apoptosis: a mechanism of acute and chronic liver injury. *Gut* **2005**, *54* (7), 1024–1033.

(2) Wang, H.; Khaoustov, V. I.; Krishnan, B.; Cai, W.; Stoll, B.; Burrin, D. G.; Yoffe, B. Total parenteral nutrition induces liver steatosis and apoptosis in neonatal piglets. *J. Nutr.* **2006**, *136* (10), 2547–2552.

(3) Strader, D. B.; Bacon, B. R.; Lindsay, K. L.; La Brecque, D. R.; Morgan, T.; Wright, E. C.; Allen, J.; Khokar, M. F.; Hoofnagle, J. H.; Seeff, L. B. Use of complementary and alternative medicine in patients with liver disease. *Am. J. Gastroenterol.* **2002**, *97* (9), 2391–2397.

(4) Divisi, D.; Di, T. S.; Salvemini, S.; Garramone, M.; Crisci, R. Diet and cancer. *Acta Biomed.* **2006**, *77* (2), 118–123.

(5) Sweeney, M. I.; Kalt, W.; MacKinnon, S. L.; Ashby, J.; Gottschall-Pass, K. T. Feeding rats diets enriched in lowbush blueberries for six weeks decreases ischemia-induced brain damage. *Nutr. Neurosci.* **2002**, *5* (6), 427–431.

(6) Baur, J. A.; Pearson, K. J.; Price, N. L.; Jamieson, H. A.; Lerin, C.; Kalra, A.; Prabhu, V. V.; Allard, J. S.; Lopez-Lluch, G.; Lewis, K.; Pistell, P. J.; Poosala, S.; Becker, K. G.; Boss, O.; Gwinn, D.; Wang, M.; Ramaswamy, S.; Fishbein, K. W.; Spencer, R. G.; Lakatta, E. G.; Le, C. D.; Shaw, R. J.; Navas, P.; Puigserver, P.; Ingram, D. K.; de, C. R.; Sinclair, D. A. Resveratrol improves health and survival of mice on a high-calorie diet. *Nature* **2006**, *444* (7117), 337–342.

(7) Ye, X.; Krohn, R. L.; Liu, W.; Joshi, S. S.; Kuszynski, C. A.; McGinn, T. R.; Bagchi, M.; Preuss, H. G.; Stohs, S. J.; Bagchi, D. The cytotoxic effects of a novel IH636 grape seed proanthocyanidin extract on cultured human cancer cells. *Mol. Cell. Biochem.* **1999**, *196* (1−2), 99–108.
(8) Choan, E.; Segal, R.; Jonker, D.; Malone, S.; Reaume, N.; Eapen, L.; Gallant, V. A prospective clinical trial of green tea for hormone refractory prostate cancer: an evaluation of the complementary/alternative therapy approach. *Urol. Oncol.* **2005**, *23* (2), 108–113.
(9) Kuriyama, S. The relation between green tea consumption and cardiovascular disease as evidenced by epidemiological studies. *J. Nutr.* **2008**, *138* (8), 1548S–1553S.
(10) Hu, G.; Tuomilehto, J.; Pukkala, E.; Hakulinen, T.; Antikainen, R.; Vartiainen, E.; Jousilahti, P. Joint effects of coffee consumption and serum gamma-glutamyltransferase on the risk of liver cancer. *Hepatology* **2008**, *48* (1), 129–136.
(11) Ortiz, D.; Shea, T. B. Apple juice prevents oxidative stress induced by amyloid-beta in culture. *J. Alzheimers. Dis.* **2004**, *6* (1), 27–30.
(12) German, J. B.; Walzem, R. L. The health benefits of wine. *Annu. Rev. Nutr.* **2000**, *20*, 561–593.
(13) Ajmo, J. M.; Liang, X.; Rogers, C. Q.; Pennock, B.; You, M. Resveratrol alleviates alcoholic fatty liver in mice. *Am. J. Physiol. Gastrointest. Liver Physiol.* **2008**, *295* (4), G833–G842.
(14) Davies, M. J.; Baer, D. J.; Judd, J. T.; Brown, E. D.; Campbell, W. S.; Taylor, P. R. Effects of moderate alcohol intake on fasting insulin and glucose concentrations and insulin sensitivity in postmenopausal women: a randomized controlled trial. *JAMA−J. Am. Med. Assoc.* **2002**, *287* (19), 2559–2562.
(15) Dunn, W.; Xu, R.; Schwimmer, J. B. Modest wine drinking and decreased prevalence of suspected nonalcoholic fatty liver disease. *Hepatology* **2008**, *47* (6), 1947–1954.
(16) Fuhrman, B.; Volkova, N.; Coleman, R.; Aviram, M. Grape powder polyphenols attenuate atherosclerosis development in apolipoprotein E deficient (E0) mice and reduce macrophage atherogenicity. *J. Nutr.* **2005**, *135* (4), 722–728.
(17) Gresele, P.; Pignatelli, P.; Guglielmini, G.; Carnevale, R.; Mezzasoma, A. M.; Ghiselli, A.; Momi, S.; Violi, F. Resveratrol, at concentrations attainable with moderate wine consumption, stimulates human platelet nitric oxide production. *J. Nutr.* **2008**, *138* (9), 1602–1608.
(18) Delmas, D.; Rebe, C.; Lacour, S.; Filomenko, R.; Athias, A.; Gambert, P.; Cherkaoui-Malki, M.; Jannin, B.; Dubrez-Daloz, L.; Latruffe, N.; Solary, E. Resveratrol-induced apoptosis is associated with Fas redistribution in the rafts and the formation of a death-inducing signaling complex in colon cancer cells. *J. Biol. Chem.* **2003**, *278* (42), 41482–41490.
(19) Aggarwal, B. B.; Shishodia, S. Molecular targets of dietary agents for prevention and therapy of cancer. *Biochem. Pharmacol.* **2006**, *71* (10), 1397–1421.
(20) Ray, S. D.; Lam, T. S.; Rotollo, J. A.; Phadke, S.; Patel, C.; Dontabhaktuni, A.; Mohammad, S.; Lee, H.; Strika, S.; Dobrogowska, A.; Bruculeri, C.; Chou, A.; Patel, S.; Patel, R.; Manolas, T.; Stohs, S. Oxidative stress is the master operator of drug and chemically-induced programmed and unprogrammed cell death: Implications of natural antioxidants in vivo. *Biofactors* **2004**, *21* (1−4), 223–232.
(21) Xie, Q.; Khaoustov, V. I.; Chung, C. C.; Sohn, J.; Krishnan, B.; Lewis, D. E.; Yoffe, B. Effect of tauroursodeoxycholic acid on endoplasmic reticulum stress-induced caspase-12 activation. *Hepatology* **2002**, *36* (3), 592–601.
(22) Puiggros, F.; Llopiz, N.; Ardevol, A.; Blade, C.; Arola, L.; Salvado, M. J. Grape seed procyanidins prevent oxidative injury by modulating the expression of antioxidant enzyme systems. *J. Agric. Food Chem.* **2005**, *53*, 6080–6086.
(23) Ren, C.; Li, L.; Goltsov, A. A.; Timme, T. L.; Tahir, S. A.; Wang, J.; Garza, L.; Chinault, A. C.; Thompson, T. C. mRTVP-1, a novel p53 target gene with proapoptotic activities. *Mol. Cell. Biol.* **2002**, *22* (10), 3345–3357.
(24) Cai, W.; Khaoustov, V. I.; Xie, Q.; Pan, T.; Le, W.; Yoffe, B. Interferon-alpha-induced modulation of glucocorticoid and serotonin receptors as a mechanism of depression. *J. Hepatol.* **2005**, *42* (6), 880–887.
(25) Ariga, A.; Namekawa, J.; Matsumoto, N.; Inoue, J.; Umezawa, K. Inhibition of tumor necrosis factor-α-induced nuclear translocation and activation of NF-κB by dehydroxymethylepoxyquinomicin. *J. Biol. Chem.* **2002**, *277* (27), 24625–24630.
(26) Fabregat, I.; Roncero, C.; Fernandez, M. Survival and apoptosis: a dysregulated balance in liver cancer. *Liver Int.* **2007**, *27* (2), 155–162.
(27) Zern, T. L.; Wood, R. J.; Greene, C.; West, K. L.; Liu, Y.; Aggarwal, D.; Shachter, N. S.; Fernandez, M. L. Grape polyphenols exert a cardioprotective effect in pre- and postmenopausal women by lowering plasma lipids and reducing oxidative stress. *J. Nutr.* **2005**, *135* (8), 1911–1917.
(28) Wang, Q.; Simonyi, A.; Li, W.; Sisk, B. A.; Miller, R. L.; MacDonald, R. S.; Lubahn, D. E.; Sun, G. Y.; Sun, A. Y. Dietary grape supplement ameliorates cerebral ischemia-induced neuronal death in gerbils. *Mol. Nutr. Food Res.* **2005**, *49* (5), 443–451.
(29) Butelli, E.; Titta, L.; Giorgio, M.; Mock, H. P.; Matros, A.; Peterek, S.; Schijlen, E. G.; Hall, R. D.; Bovy, A. G.; Luo, J.; Martin, C. Enrichment of tomato fruit with health-promoting anthocyanins by expression of select transcription factors. *Nat. Biotechnol.* **2008**, *26* (11), 1301–1308.
(30) Appel, M. J.; van Garderen-Hoetmer, A.; Woutersen, R. A. Lack of inhibitory effects of beta-carotene, vitamin C, vitamin E and selenium on development of ductular adenocarcinomas in exocrine pancreas of hamsters. *Cancer Lett.* **1996**, *103* (2), 157–162.
(31) Purohit, V.; Abdelmalek, M. F.; Barve, S.; Benevenga, N. J.; Halsted, C. H.; Kaplowitz, N.; Kharbanda, K. K.; Liu, Q. Y.; Lu, S. C.; McClain, C. J.; Swanson, C.; Zakhari, S. Role of *S*-adenosylmethionine, folate, and betaine in the treatment of alcoholic liver disease: summary of a symposium. *Am. J. Clin. Nutr.* **2007**, *86* (1), 14–24.
(32) Green, D. R.; Reed, J. C. Mitochondria and apoptosis. *Science* **1998**, *281* (5381), 1309–1312.
(33) Tyurina, Y. Y.; Serinkan, F. B.; Tyurin, V. A.; Kini, V.; Yalowich, J. C.; Schroit, A. J.; Fadeel, B.; Kagan, V. E. Lipid antioxidant, etoposide, inhibits phosphatidylserine externalization and macrophage clearance of apoptotic cells by preventing phosphatidylserine oxidation. *J. Biol. Chem.* **2004**, *279* (7), 6056–6064.
(34) Herceg, Z.; Wang, Z. Q. Functions of poly(ADP-ribose) polymerase (PARP) in DNA repair, genomic integrity and cell death. *Mutat. Res.* **2001**, *477* (1−2), 97–110.
(35) Yao, R.; Cooper, G. M. Requirement for phosphatidylinositol-3 kinase in the prevention of apoptosis by nerve growth factor. *Science* **1995**, *267* (5206), 2003–2006.

Received March 12, 2009. Revised manuscript received May 30, 2009. Accepted September 1, 2009.